Effect of Sintering Pressure on the Porosity and the Shear Strength of the Pressure-Assisted Silver Sintering Bonding

Liu, Yang; Zhang, Hao; Wang, Lingen; Fan, Xuejun; Zhang, Guoqi; Sun, Fenglian

DOI
10.1109/TDMR.2018.2819431

Publication date
2018

Document Version
Accepted author manuscript

Published in
IEEE Transactions on Device and Materials Reliability

(2018), IEEE Transactions on Device and Materials Reliability, 18(2): 240-246, doi: 10.1109/TDMR.2018.2819431

Effect of sintering pressure on the porosity and the shear strength of the pressure-assisted silver sintering bonding

Yang Liu, Hao Zhang, Lingen Wang, Xuejun Fan, *Senior Member*, *IEEE,* Guoqi Zhang, *Fellow, IEEE*, and Fenglian Sun

***Abstract*— The microstructure, thickness, porosity, and shear performance of the silver (Ag) sintering layers under different sintering pressures were investigated. Experimental results demonstrated that the thickness and the porosity of the sintering layer decreased when the sintering pressure varied from 5 MPa to 30 MPa. This densification phenomenon facilitated the enhancement of the Ag sintering layers. The shear strength was improved significantly from 44.19 MPa to 69.41 MPa when the sintering pressure increased from 5 MPa to 10 MPa. When the sintering pressure ranged from 10 MPa to 30 MPa, the shear strength presented a slow increase from 69.41 MPa to 73.38 MPa. According to the results of the failure analysis, fracture mode transformation was considered as the basic reason for this phenomenon. The increasing sintering pressure promoted the bonding of the nano-Ag particles during the sintering process. Consequently, the fracture of the sintered-Ag layer transformed from brittle fracture to ductile fracture because of the increasing sintering pressure. The delamination area between Cu and Ni layers coated on the bottom Mo plate was clearly enlarged with the increasing sintering pressure. The delamination between Cu and Ni layers coated on the bottom Mo plate turned to be the main failure mode when the sintering pressure was higher than 10 MPa.**

***Index Terms*—Reliability, sintering, porosity, strength, bonding**

I. INTRODUCTION

As the development of power electronic technology, high power chips have been widely used in automotive, energy transfer, and aerospace industries in the near decades [1-4]. The developing trend of power chips toward high voltage and high power density has become a challenge for the module design due to reliability concern [5, 6]. Meanwhile, it brings a higher requirement for the bonding technology of power chips, such as

This work was supported by National Natural Science Foundation of China (No. 51604090), Natural Science Foundation of Heilongjiang Province (No. E2017050), and University Nursing Program for Young Scholars with Creative Talents in Heilongjiang Province (UNPYSCT-2015042). *(Corresponding author: Yang Liu)*

Yang Liu, Hao Zhang, and Fenglian Sun are with the School of Materials Science and Engineering, Harbin University of Science and Technology, Harbin, 150040 China (e-mail: lyang805@163.com).

Lingen Wang is with Boschman Technologies B.V., Duiven, Netherlands.

Xuejun Fan is with Department of Mechanical Engineering, Lamar University, Beaumont, USA.

Guoqi Zhang is with the EEMCS Faculty, Delft University of Technology, Delft, Netherlands.

high-temperature service, high bonding strength, long reliability etc.

Traditional bonding method of power chips includes conductive adhesive bonding, wire bonding, soldering etc [7-9]. Adhesive bonding and wire bonding cannot be used in high-power applications due to their poor bonding strength, electrical and thermal conductivities. Considering these properties, soldering is better than the bonding methods. However, there are some disadvantages of soldering which restrict its application in high-power bonding [10, 11]. One of the critical problems is the IMC evolution at the soldering interfaces [12, 13], which is a potential threat to the reliability of the whole module. It is a critical issue, especially for the applications in automotive and aerospace industries. Due to reliability concern, sintering is considered as a promising method for the assembly of power chips [14].

As a replacement of soldering in high temperature applications, silver (Ag) sintering has drawn increasing attention to the bonding of power modules as well as other electronic devices [15-19]. Compared with Pb-Sn and Au-based solder alloys, Ag shows much higher thermal conductivity and electrical conductivity [20]. In the research by Hutzler et al [21], the samples by Ag sintering shows much longer life time than that by Pb-Sn soldering during the power cycling tests. Though Ag has significant advantages on the physical and the mechanical properties, it is difficult to achieve the theoretical performances of Ag by solid sintering method of Ag nanoparticles. Bordia et al [22] reviews the fundamentals of sintering process. Due to the geometrical effect of the nanoparticles, the particle neck and pores suppress the properties of the sintering layer. An effective way to decrease the porosity in the sintering layer is to add external pressure during the sintering process. Lu et al [23] reported that the 5 MPa pressure significantly promoted the microstructure densification, and consequently increased the shear strength of the Ag sintering layer. Besides, the decreasing porosity also has positive effects on the thermal and electrical performance of the sintering layers. Therefore, pressure-assisted Ag sintering has become the developing trend and been used in industry.

Currently, the typical sintering pressure used in industry ranges from 5 MPa to 30 MPa. It is commonly believed that the sintering pressure should be as high as possible to obtain high-quality bonding [24]. However, high sintering pressure aggravates the chances of chip failure. It is of great significance to enrich the theoretical basis to design the sintering parameters in pressure-assisted sintering process. In this study, the effect of sintering pressure on the porosity and the shear strength of the bonding surfaces was investigated. Moreover, the fracture modes of the specimens under different sintering pressures were analyzed.

II. EXPERIMENTS

Figure 1 (a) shows a commercially available pressure-assisted sintering equipment (Sinterstar, Boschman Technologies B.V.) used in this study. The sintering substrates are molybdenum (Mo) plates (13.6 × 13.6 × 2 mm). The dummy dies used in this study are smaller Mo plates (9.4 × 9.4 × 1.2 mm). The Mo plates are coated with Ni/Cu/Ag surface layers by electroless plating deposition. Here the thickness of Ni, Cu, and Ag layers are 1, 1, and 3 μm respectively. surface layers which is 5μm thick. coated with Ag. The sintering material is ALPHA Argomax nano-Ag film with the thickness of 65 μm. The nano-Ag film

is made with nano Ag particles. The top and the bottom Mo plates were fixed by a specially-designed fixture during the sintering process in order to guarantee the dimensional consistency of all the sintering specimens. The sintering temperature was 250 ℃, and the sintering time was 3 mins. The sintering pressure was 5, 10, 20, and 30 MPa, respectively. The specimens are as shown in Fig.1 (b). The structure of the specimen can be seen in the schematic diagram presented in Fig.1 (c).

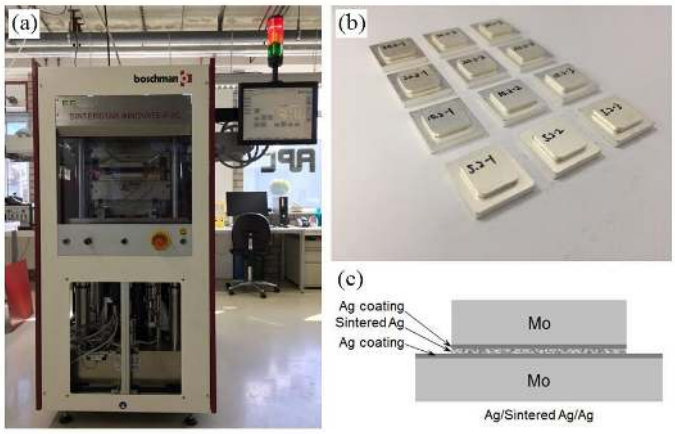

Fig.1 Sintering equipment and specimens: (a) Pressure-assisted sintering equipment, (b) sintering specimens, and (c) schematic diagram of the sintering structure

In order to investigate the porosity and microstructure of the sintering layers, cross-sectional grind and polishing were carefully conducted and then ultrasonic clean was implemented. Here the grid and polishing papers were 500, 1000, 1500, 2000, and 3500#. The ultrasonic clean process was used to clean the polished Ag and impurities at the surfaces. The microstructure of the sintering layers were characterized by FEI scanning electron microscope (SEM) and energy dispersive X-ray spectroscope (EDS). Meanwhile, the porosity of each specimen was calculated based on visible void areas from the cross-sectional view. The shear strength of the specimens was evaluated by the Instron 5569 mechanical tester with a specially-designed fixture as shown in the Figures 2 (a) and (b). The shear speed was 0.3 mm/min. The schematic diagram of the shear test is presented in Fig.2 (c). SEM was used to observe the morphology of the shear fractured locations. The elemental analysis of the area of interest on these locations was characterized by EDS.

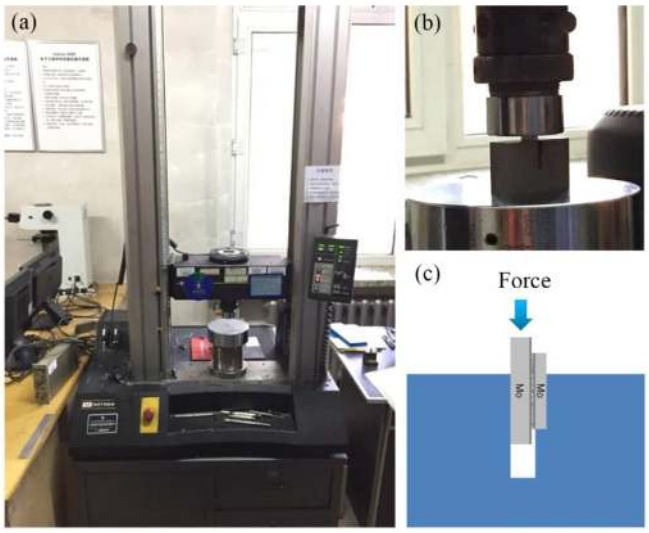

Fig.2 Shear tester and fixture: (a) Instron 5569 mechanical tester, (b) fixture designed for the specimens, and (c) schematic diagram of the shear test

III. RESULTS AND DISCUSSION

Fig. 3 shows the Cross-sectional SEM micrographs of the sintering interfaces under the sintering pressures of 5, 10, 20, and 30 MPa, respectively. The dark layer next to the Mo layer, which consists of two elements, Ni and Cu, is formed of Ni-coated layer on the Mo plate and Cu-coated layer on Ni coated layer. Here the total thickness of the Ni and the Cu layers is about 2 μm. The layer next to the Cu layer is the Ag-coated layer exposed to air of the Mo substrate. The thickness of this Ag-coated layer is about 5 μm.

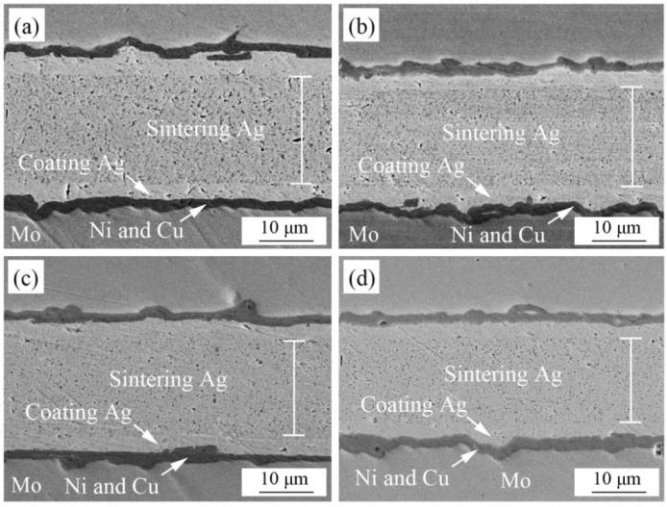

Fig.3 Cross-sectional SEM micrographs of the sintering interfaces under the sintering pressures of: (a) 5 MPa, (b) 10 MPa, (c) 20 MPa, and (d) 30 MPa

As shown in Fig.3, the sintered Ag layer is located between the two Ag-coated layers. The thickness of the sintered Ag layers is marked by the white lines in the figures. The result of the EDS line scan as shown in Fig.4 indicates that the top and the bottom layers

are Mo. It is clear that the sintering pressure has significant effects on the thickness of the sintering layers. The thickness of the sintering layers is calculated according to the ratio of the measured data to the scale. As presented in Fig.5, the thickness of the sintering layer is 20.38 μm under the sintering pressure of 5 MPa. The thickness shows a decreasing trend while the sintering pressure increases. As the sintering pressure reaches 30 MPa, the thickness of the sintering layer decreases to 16.15 μm.

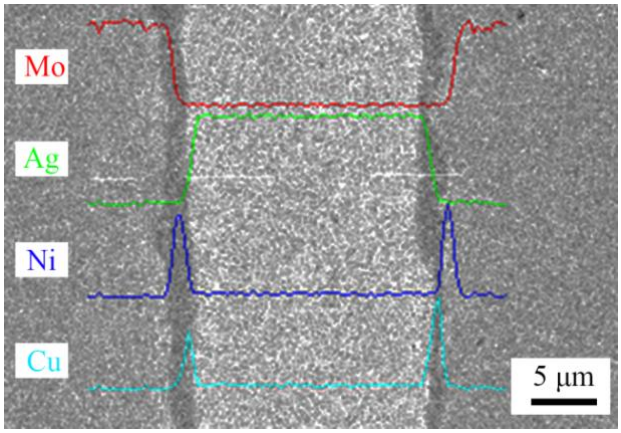

Fig.4 EDS line scan result of the sintering interface

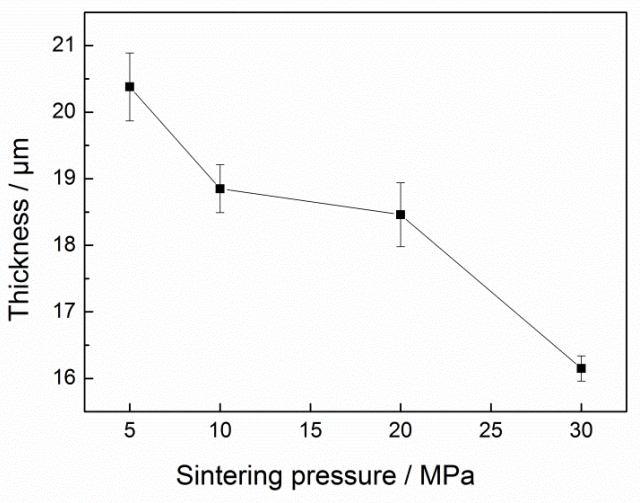

Fig.5 Thickness of the sintered Ag layers

Because the volume of void space in the sintering layer is in nano scale in this study, it is hard to characterize the porosity by X-ray observation because its resolution of X-ray is not high enough for nano voids. Therefore, the porosity of the sintering layers were calculated on the basis of the SEM micrographs. As shown in Fig.6, the black area represents the void in the microstructure. The area of the void can be calculated using AutoCAD software. Then the porosity of each specimen was obtained.

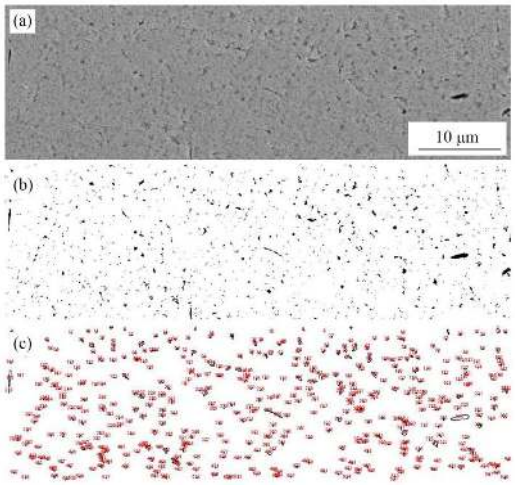

Fig.6 Calculation of the porosity in the sintered Ag layer. (a) SEM morphology, (b) gradation processing, and (c) area calculation

Fig.7 shows the porosity of the sintering layers under various sintering pressures. As presented in the figure, the transforming tendency of the porosity is similar to the change of thickness due to the increase of sintering pressure. The porosity of the sintering layer decreases from 1.39% to 1.14% as the sintering pressure rises from 5 MPa to 30 MPa. Therefore, high sintering pressure facilitates the densification of the sintering layer. Here the values are lower than that of about 10% in the publications by Kähler et al [25]. The reason is that the bonding material used in this study is a commercial nano-Ag film. Compared with nano-Ag paste, nano-Ag film has higher density which is helpful to decrease the porosity of the sintered layers. Zhao et al [26] also obtained the sintered layer whose porosity is lower than 10% using similar Ag film on DBC substrate.

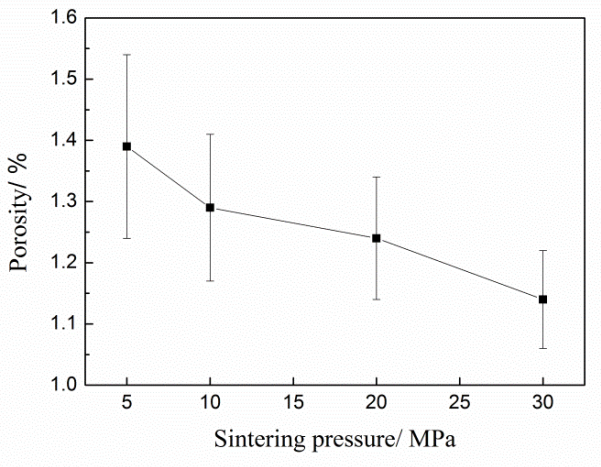

Fig.7 Porosity in the sintered Ag layers

Fig.8 shows the shear strength of the sintering specimens under different sintering pressures. As shown in the figure, the shear strength is about 44.19 MPa when the sintering pressure is 5 MPa. A significant increase of the shear strength appears and reaches 69.41 MPa as the sintering pressure increases to 10 MPa. When the sintering pressure ranges

from 10 MPa to 30 MPa, the shear strength presents a slow increase. The value of the strength is about 73.38 MPa when the sintering pressure is 30 MPa. As discussed, the increasing of sintering pressure improves the density of the sintered layer. The deformation of the Ag nano particles enlarges the contact area among the particles. High sintering pressure is considered to be helpful for the solid diffusion at the interfaces. Consequently, the bonding quality was improved.

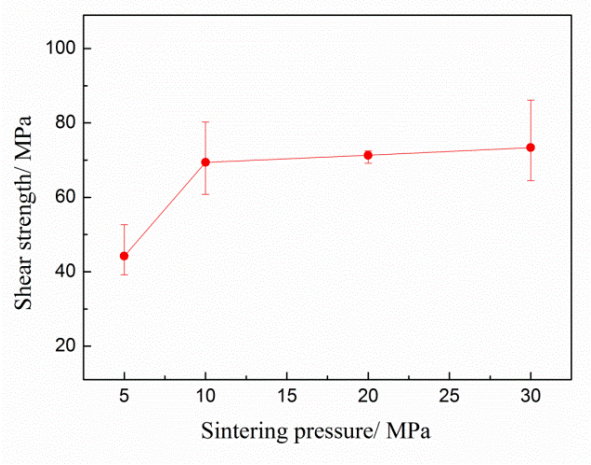

Fig.8 Shear strength of the sintering specimens

The SEM morphology and EDS analysis of the shear fracture under 5 MPa sintering pressure can be observed in Fig.9. As shown in Fig.9 (a), the top Mo plates were peeled off during the shear test. The SEM micrograph of the red area in Fig.9 (a) is as shown in Fig.9 (b). The morphology of this fracture consists of two kinds of the surfaces. The EDS results in Fig.9 (d) and (e) demonstrate that the gray area is the fracture of the sintered Ag, while the dark area represents the Ni layer coated on the bottom Mo plate. Here the Ti element is due to the testing deviation of the EDS equipment or the impurity of the Mo plate. The magnified micrograph of the selected area in Fig.9 (c) shows the morphology of the shear fracture of the sintered Ag. Ag nano particles with the diameter of about 500 nm can be distinctly observed in this figure. Meanwhile, some of the coated Ag layer was removed. Therefore, the fracture mode of the specimens under the sintering pressure of 5 MPa includes two types of fracture during the shear test. One is the brittle fracture between the nano Ag particles in the sintering layer. The other one is the delamination between the Cu and Ni layers coated on the bottom Mo plate. The delamination can be clearly observed from the morphology and EDS line scan analysis as shown in Fig.10.

Fig.11 shows the SEM morphology and EDS analysis of the shear fracture when the sintering pressure is 30 MPa. Compared with shear fracture under 5 MPa sintering pressure in Fig.9, the delamination area between the Cu and Ni layers coated on the bottom Mo plate significantly increases. As shown in Fig.11 (b), only small area of Ag fracture can be observed. The magnified fracture is presented in Fig.11 (c). It is obvious that the fracture in the sintered Ag is mainly due to the ductile failure of Ag layer. Therefore, the failure of the specimens under 30 MPa sintering pressure is mainly due to the delamination between the Cu and Ni layers coated on the bottom Mo plate during the shear test. Meanwhile, minor area resembles as a ductile fracture within the sintered Ag film.

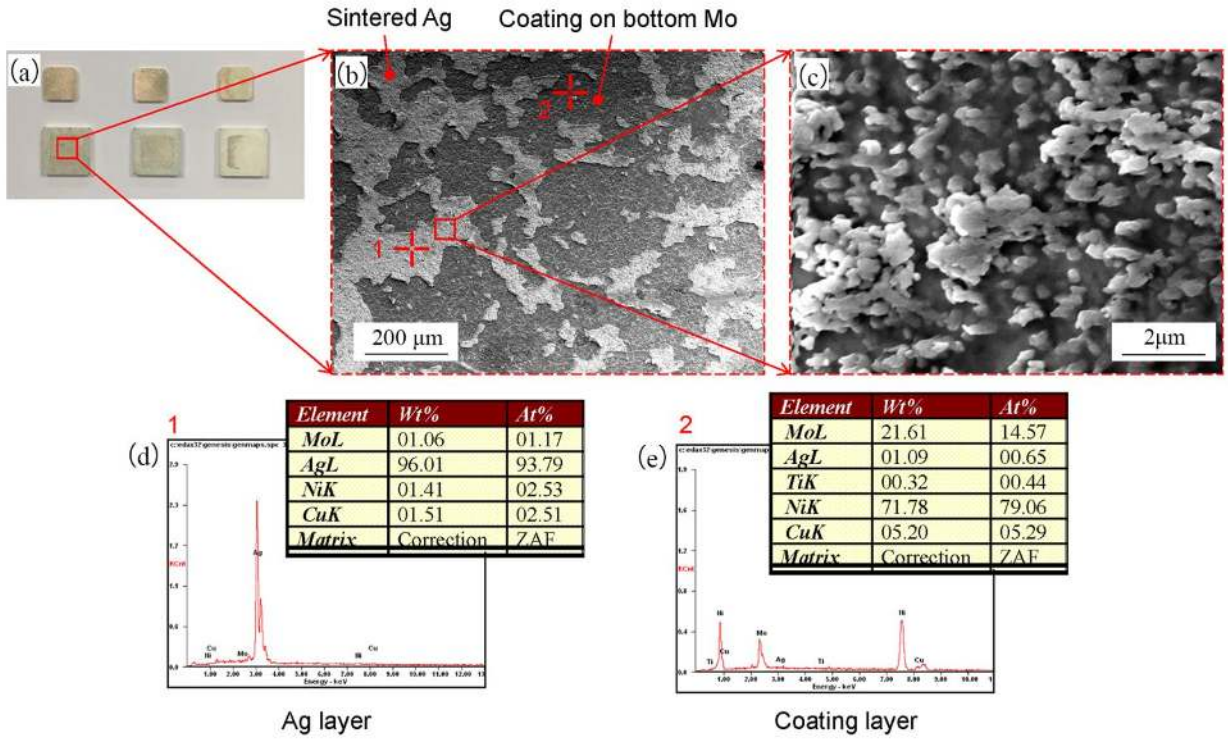

1	Element	Wt%	At%
	MoL	01.06	01.17
	AgL	96.01	93.79
	NiK	01.41	02.53
	CuK	01.51	02.51
	Matrix	Correction	ZAF

2	Element	Wt%	At%
	MoL	21.61	14.57
	AgL	01.09	00.65
	TiK	00.32	00.44
	NiK	71.78	79.06
	CuK	05.20	05.29
	Matrix	Correction	ZAF

Fig.9 Morphology and EDS analysis of the shear fracture under 5 MPa sintering pressure. (a) optical micrograph of the sheared specimens, (b) SEM micrograph of the shear fracture, (c) magnified area of (b), (d) EDS result of point 1 in (b), (e) EDS result of point 2 in (b)

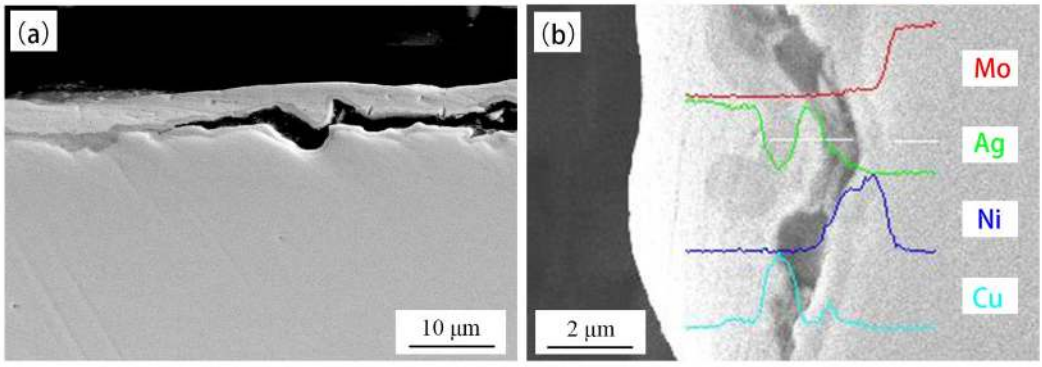

Fig.10 Morphology and EDS line scan analysis of the delamination

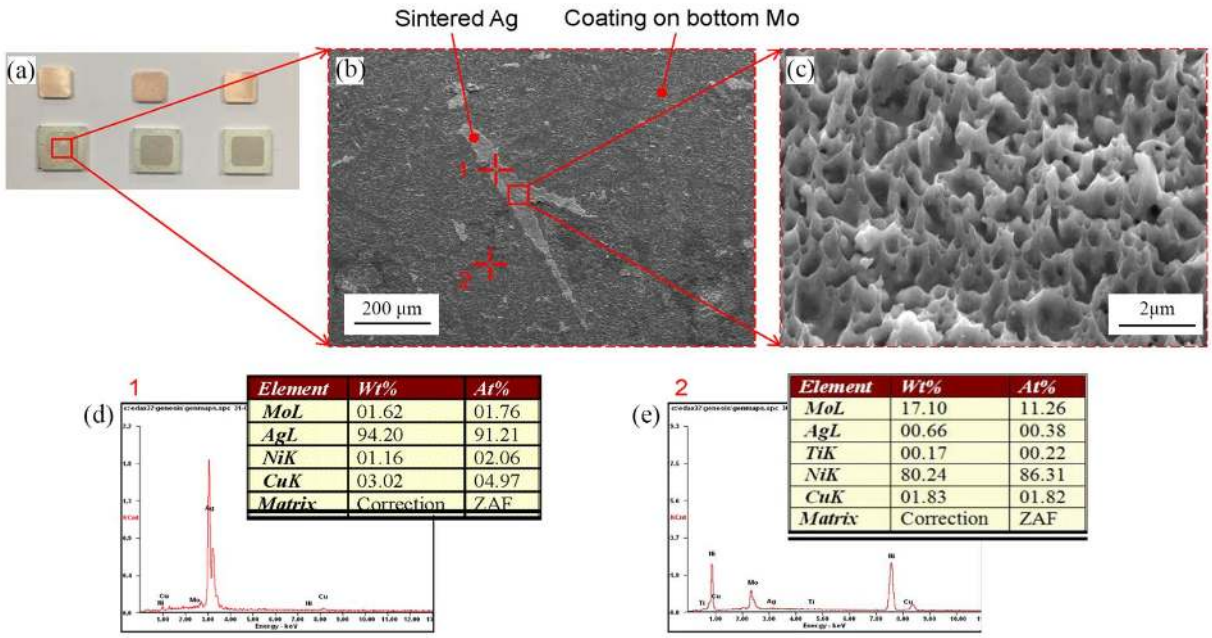

Element	Wt%	At%
MoL	01.62	01.76
AgL	94.20	91.21
NiK	01.16	02.06
CuK	03.02	04.97
Matrix	Correction	ZAF

Element	Wt%	At%
MoL	17.10	11.26
AgL	00.66	00.38
TiK	00.17	00.22
NiK	80.24	86.31
CuK	01.83	01.82
Matrix	Correction	ZAF

Fig.11 Morphology and EDS analysis of the shear fracture under 30 MPa sintering pressure. (a) optical micrograph of the sheared specimens, (b) SEM micrograph of the shear fracture, (c) magnified area of (b), (d) EDS result of point 1 in (b), (e) EDS result of point 2 in (b)

Fig.12 shows the magnified morphology of the shear fractures of the sintered Ag under the sintering pressures of 5, 10, 20, and 30 MPa, respectively. As shown in the figure, the Ag sintered layer experiences brittle failure when the sintering pressure is 5 MPa. As the sintering pressure ranges from 10 to 30 MPa, the fracture modes are ductile failure. The transformation from brittle to ductile mode of fractures is considered as the reason why the shear strength appears a sharp increase due to the increase of sintering pressure from 5 to 30 MPa. As the sintering pressure reaches 10 MPa, significant improvement (~57%) in the shear strength of sintering layer is observed. In contrast, the interface between the Ni/Cu coated layers over Mo turns out to be the weakest link in the whole package. Therefore, although clear densification appears when the sintering pressure increases from 10 to 30 MPa, the shear strength does not show an obvious enhancement. In order to obtain further improvement on the bonding strength of the whole module, it is necessary to conduct more studies on the materials and the coating processes of adhesion layers.

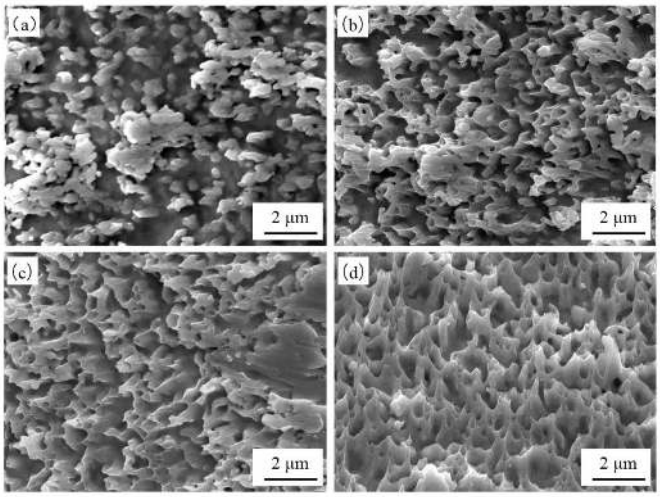

Fig.12 Magnified morphology of the shear fractures of the sintered Ag under the sintering pressures of: (a) 5 MPa, (b) 10 MPa, (c) 20 MPa, and (d) 30 MPa

IV. Conclusion

1. Increasing the sintering pressure facilitates the densification of the sintered Ag layer. As the sintering pressure rises from 5 MPa to 30 MPa, the thickness and the porosity of the sintered layer decrease by 20.75% and 17.99% respectively.
2. The shear strength grows significantly from 44.19 MPa to 69.41 MPa when the sintering pressure increases from 5 MPa to 10 MPa. Further increase of the sintering pressure shows limited enhancement on the shear strength in this study.
3. The fracture mode of the specimens under the sintering pressure of 5 MPa includes two types of fracture during the shear test. One is the brittle fracture between the nano Ag particles in the sintering layer. The other one is the delamination between the Cu and Ni layers coated on the bottom Mo plate.
4. As the sintering pressure increases from 5 MPa to 30 MPa, the shear fracture of sintered Ag transformed from brittle fracture to ductile fracture. Delamination between the Cu and the Ni layers coated on the bottom Mo plate turns to be the main fracture mode when the sintering pressure is higher than 10 MPa.
5. Future works will focus on the reliability evaluation such as the thermal cycling and high temperature aging tests for the real power modules. Meanwhile, the other properties such as thermal and electrical performances of the sintered nano-Ag film will be of interest for investigation.

References

[1] M. Gleissner and M. M. Bakran, "Design and control of fault-tolerant nonisolated multiphase multilevel DC–DC converters for automotive power systems," IEEE Transactions on Industry Applications, vol. 52, pp. 1785-1795, 2016.

[2] M. A. Khan, I. Husain, and Y. Sozer, "A bidirectional dc–dc converter with overlapping input and output voltage ranges and vehicle to grid energy transfer capability," IEEE Journal of Emerging and Selected Topics in Power Electronics, vol. 2, pp. 507-516, 2014.

[3] Y. Peng, P. Sun, L. Zhou, X. Du, and J. Cai, "A temperature-independent method for monitoring the degradation of bond wires in IGBT modules based on transfer characteristics," in Applied Power Electronics Conference and Exposition (APEC), 2017 IEEE, 2017, pp. 751-755.

[4] F. Yu, R. W. Johnson, and M. C. Hamilton, "Process Optimization of Pressure-Assisted Rapid Ag Sintering Die Attach for 300° C Applications," IEEE Transactions on Components, Packaging and Manufacturing Technology, vol. 7, pp. 855-861, 2017.

[5] P. Ghimire, A. R. de Vega, S. Beczkowski, B. Rannestad, S. Munk-Nielsen, and P. Thogersen, "Improving power converter reliability: Online monitoring of high-power IGBT modules," IEEE Industrial Electronics Magazine, vol. 8, pp. 40-50, 2014.

[6] H. Luo, Y. Chen, P. Sun, W. Li, and X. He, "Junction temperature extraction approach with turn-off delay time for high-voltage high-power IGBT modules," IEEE Transactions on Power Electronics, vol. 31, pp. 5122-5132, 2016.

[7] Y. Mei, G. Chen, Y. Cao, X. Li, D. Han, and X. Chen, "Simplification of low-temperature sintering nanosilver for power electronics packaging," Journal of electronic materials, vol. 42, pp. 1209-1218, 2013.

[8] Y. Liu, J. Zhao, C. C.-A. Yuan, G. Q. Zhang, and F. Sun, "Chip-on-flexible packaging for high-power flip-chip light-emitting diode by AuSn and SAC soldering," IEEE Transactions on Components, Packaging and Manufacturing Technology, vol. 4, pp. 1754-1759, 2014.

[9] D. Gross, S. Haag, M. Reinold, M. Schneider-Ramelow, and K.-D. Lang, "Heavy copper wire-bonding on silicon chips with aluminum-passivated Cu bond-pads," Microelectronic Engineering, vol. 156, pp. 41-45, 2016.

[10] R. Berni, M. Catelani, C. Fiesoli, and V. L. Scarano, "A Comparison of Alloy-Surface Finish Combinations Considering Different Component Package Types and Their Impact on Soldering Reliability," IEEE Transactions on Reliability, vol. 65, pp. 272-281, 2016.

[11] D. A. Shnawah, M. F. M. Sabri, and I. A. Badruddin, "A review on thermal cycling and drop impact reliability of SAC solder joint in portable electronic products," Microelectronics reliability, vol. 52, pp. 90-99, 2012.

[12] W.-H. Chen, C.-F. Yu, H.-C. Cheng, Y.-m. Tsai, and S.-T. Lu, "IMC growth reaction and its effects on solder joint thermal cycling reliability of 3D chip stacking packaging," Microelectronics Reliability, vol. 53, pp. 30-40, 2013.

[13] Y. Liu, F. Sun, H. Zhang, T. Xin, C. A. Yuan, and G. Zhang, "Interfacial reaction and failure mode analysis of the solder joints for flip-chip LED on ENIG and Cu-OSP surface finishes," Microelectronics Reliability, vol. 55, pp. 1234-1240, 2015.

[14] S. A. Paknejad and S. H. Mannan, "Review of silver nanoparticle based die attach materials for high power/temperature applications," Microelectronics Reliability, 2017.

[15] M. Barrière, A. Guédon-Gracia, E. Woirgard, S. Bontemps, and F. Le Henaff, "Innovative conception of SiC MOSFET-Schottky 3D power inverter module with double side cooling and stacking using silver sintering," Microelectronics Reliability, vol. 76, pp. 431-437, 2017.

[16] D. E. Xu, J. B. Kim, M. D. Hook, J. P. Jung, and M. Mayer, "Real time resistance monitoring during sintering of silver paste," Journal of Alloys and Compounds, vol. 731, pp. 504-514, 2018.

[17] J. Kähler, A. Stranz, A. Waag, and E. Peiner, "Thermoelectric coolers with sintered silver interconnects." Journal of Electronic Materials, vol. 43, pp. 2397-2404, 2014.

[18] A. Stranz, A. Waag, and E. Peiner, "Investigation of Thermoelectric Parameters of Bi 2 Te 3: TEGs Assembled using Pressure-Assisted Silver Powder Sintering-Based Joining Technology." Journal of Electronic Materials, vol. 44, pp. 2055-2060, 2015.

[19] H. Li, H. Jing, Y. Han, G. Q. Lu, L. Xu, and T. Liu, "Interface evolution analysis of graded thermoelectric materials joined by low temperature sintering of nano-silver paste." Journal of Alloys and Compounds, vol. 659, pp. 95-100, 2016.

[20] F. Le Henaff, S. Azzopardi, J. Y. Deletage, E. Woirgard, S. Bontemps, and J. Joguet, "A preliminary study on the thermal and mechanical performances of sintered nano-scale silver die-attach technology depending on the substrate metallization," Microelectronics Reliability, vol. 52, pp. 2321-2325, 2012.

[21] A. Hutzler, A. Tokarski, S. Kraft, S. Zischler, and A. Schletz, "Increasing the lifetime of electronic packaging by higher temperatures: Solders vs. silver sintering," in Electronic Components and Technology Conference (ECTC), 2014 IEEE 64th, 2014, pp. 1700-1706.

[22] R. K. Bordia, S.-J. L. Kang, and E. A. Olevsky, "Current understanding and future research directions at the onset of the next century of sintering science and technology," Journal of the American Ceramic Society, vol. 100, pp. 2314-2352, 2017.

[23] G. Q. Lu, M. H. Zhao, G. Y. Lei, J. N. Calata, X. Chen, and S. Luo, "Emerging Lead-free, High-temperature Die-attach Technology Enabled by Low-temperature Sintering of Nanoscale Silver Pastes," 2009 International Conference on Electronic Packaging Technology & High Density Packaging (Icept-Hdp 2009), pp. 385-+, 2009.

[24] T. Watanabe, N. Nakajima, and M. Takesue, "Material Design and Process Conditions of Pressureless Sintered Silver for 200/-40° C Thermal Cycling Reliability," in PCIM Europe 2017; International Exhibition and Conference for Power Electronics, Intelligent Motion, Renewable Energy and Energy Management; Proceedings of, 2017, pp. 1-4.

[25] J. Kähler, N. Heuck, G. Palm, A. Stranz, A. Waag, and E. Peiner, "Low-pressure sintering of silver micro-and nanoparticles for a high temperature stable Pick & Place die attach," in 18th European Microelectronics and Packaging Conference (EMPC), 2011, pp. 1-7.

[26] Y. Zhao, P. Mumby-Croft, S. Jones, A. Dai, Z. Dou, Y. Wang, and F. Qin, "Silver sintering die attach process for IGBT power module production." in Applied Power Electronics Conference and Exposition (APEC), 2017, pp. 3091-3094.

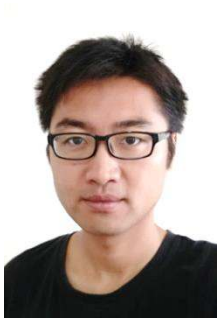

Yang Liu received the B.S. degree in materials chemistry from Lanzhou University, Lanzhou, China, in 2007, and the M.S. degree in materials processing engineering and the Ph.D. degree in materials science from the Harbin University of Science and Technology, Harbin, China, in 2010 and 2012, respectively. He is currently a Lecturer with the Department of Materials Science and Engineering, Harbin University of Science and Technology. Now he works as a guest researcher in Delft University of Technology, Delft, the Netherlands. His current research interests include LED packaging, lead-free solder materials and power electronics packaging.

He has published over 40 scientific papers. As the Principal Leader, he undertook 6 projects including the National Natural Science Foundation of China, China Postdoctoral Science Foundation, Natural Science Foundation of Heilongjiang Province.

Hao Zhang received his B.S. degree and M.S. degree from Harbin University of Science and Technology in 2013 and in 2015 respectively. Now he is pursuing his PhD degree at Beijing Research Centre of Delft University of Technology in Microelectronics.

His main research interests include the modification of lead free solders for microelectronic packaging, die-attach materials for power semiconductor packaging, as well as the reliability assessment and failure mechanism analysis of electronic components. He has worked in Boschman Technologies since July 2016, and mainly focuses on the sintering and molding process of power devices. He has participated in one National high technology research and development program (863 Project).

Lingen Wang received his Ph.D. degree from Delft University of Technology in 2008. Now he is the manager of technical developing department in Boschman Technologies B.V., the Netherlands. He has rich experiences on the product and process development for advanced electronic packaging. His current developing fields include the sintering and molding for high-power electronics, packaging for MEMS and sensors, and 3-D integration packaging.

Xuejun Fan (SM'06) received the B.S. and M.S. degree in Applied Mechanics from Tianjin University, Tianjin, China, in 1984 and 1986, respectively, and the Ph.D. degree in Solid Mechanics from Tsinghua University, Beijing, China, in 1989.

He is a Professor in the Department of Mechanical Engineering at Lamar University, Beaumont, Texas, and also a visiting professor with State Key Lab of Solid State Lighting in China. His current research interests lie in the areas of design, modeling, material characterization, and reliability in heterogeneous electronic systems. He was a Senior Staff Engineer at Intel Cooperation, Chandler, Arizona, from 2004 to 2007, a Senior Member Research Staff with Philips Research Lab at Briarcliff Manor, New York from 2001 to 2004, and a Member Technical Staff and Group Leader at the Institute of Microelectronics (IME), Singapore from 1997 to 2000. In his earlier career, he was promoted to a full professor at age 27 in 1991 at Taiyuan University of Technology, Shanxi, China, and became one of the youngest full professors in China that time.

He has published over 200 technical papers, many book chapters, and three books, and several patents. Dr. Fan received IEEE Components Packaging and Manufacturing Technology (CPMT) Society Exceptional Technical Achievement Award in 2011, and won the Best Paper Award of IEEE Transactions on Components and Packaging Technologies in 2009. He is an IEEE CPMT Distinguished Lecturer.

Guoqi Zhang (M'03–F'14) received the Ph.D. degree in aerospace engineering from Delft University of Technology, Delft, The Netherlands, in 1993.

Since 2013, he has been a Chair Professor with the Department of Microelectronics, Delft University of Technology. He had been with Philips for 20 years as Principal Scientist (1994–1996), Technology Domain Manager (1996–2005), Senior Director of Technology Strategy (2005–2009), and Philips Fellow (2009–2013). He also had part time appointments as a Professor at the Technical University of Eindhoven (2002–2005), and as a Chair Professor at Delft University of Technology (2005–2013). He is one of the pioneers in developing the "More than Moore" (MtM) strategy when he served as a Chair of MtM Technology team of

European's Nanoelectronics Platform in 2005. He has published more than 400 papers including more than 150 journal papers, 3 books, 17 book chapters, and more than 100 patents. His research interests include heterogeneous micro/nanoelectronics packaging, system integration, and reliability.

Prof. Zhang received the "Outstanding Contributions to Reliability Research" Award from the European Center for Micro/Nanoreliability, in 2007, the "Excellent Leadership Award" at EuroSimE, "Special Achievement Award" at ICEPT, and the IEEE Components, Packaging, and Manufacturing Technology Society Outstanding Sustained Technical Contribution Award in 2015.

Fenglian Sun received the B.S. and Ph.D. degrees in welding engineering and materials processing engineering from the Harbin Institute of Technology, Harbin, China. She is currently the Principal Academic Leader and Ph.D. Supervisor of Materials Processing Engineering with the School of Materials Science and Engineering, Harbin University of Science and Technology, Harbin. Prof. Sun is one of the Directors of the Material Branch of the Chinese Society for Stereology, a Board Member of the Brazing and Special Welding Branch of the China Welding Association, and a Board Member of Higher Education of the Mechanical and Electronic Branch Board of the Association of Mechanical Engineering Education. As the Principal Leader, she undertook 10 projects supported by the National Natural Science Foundation of China, the State Key Laboratory Foundation, the main project of the Natural Science Foundation of Heilongjiang Province, and the Science and Technology Bureau of Harbin.